Title

Experimental and Theoretical Evidence for Nitrogen–Fluorine Halogen Bonding in Silver-Initiated Radical Fluorinations

Journal

ACS Catalysis, 9(4)

ISSN

2155-5435

Authors

Hua, Alyssa M
Bidwell, Samantha L
Baker, Sarah I
et al.

Publication Date

2019-04-05

DOI

10.1021/acscatal.9b00623

Peer reviewed

ACS Catalysis

Letter

pubs.acs.org/acscatalysis

Experimental and Theoretical Evidence for Nitrogen−Fluorine Halogen Bonding in Silver-Initiated Radical Fluorinations

Alyssa M. Hua,[§,†] Samantha L. Bidwell,[§,†] Sarah I. Baker,[§] Hrant P. Hratchian,[*,§] and Ryan D. Baxter[*,§]

[§]Department of Chemistry and Chemical Biology, University of California, 5200 N. Lake Road, Merced, California 95343, United States

Supporting Information

ABSTRACT: We report experimental and computational evidence for nitrogen−fluorine halogen bonding in Ag(I)-initiated radical C−H fluorinations. Simple pyridines form $[N-F-N]^+$ halogen bonds with Selectfluor to facilitate single-electron reduction by catalytic Ag(I). Pyridine electronics affect the extent of halogen bonding, leading to significant differences in selectivity between mono- and difluorinated products. Electronic structure calculations show that halogen bonding to various pyridines alters the single-electron reduction potential of Selectfluor, which is consistent with experimental electrochemical analysis. Multinuclear correlation NMR also provides spectroscopic evidence for pyridine halogen bonding to Selectfluor under ambient conditions.

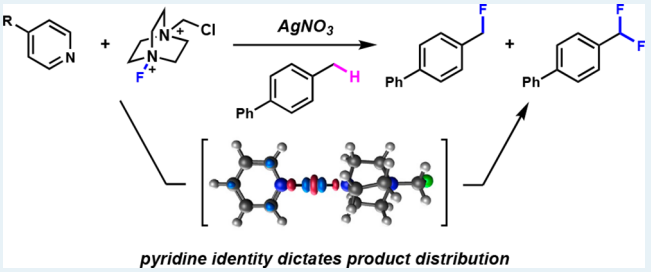

KEYWORDS: *halogen-bonding, fluorination, H atom abstraction, HAT, radical*

Noncovalent bonding interactions are broadly important to the field of organic chemistry. Electrostatic interactions including van der Waals forces, $\pi-\pi$ stacking, ion-π interactions, and hydrogen bonding are all capable of modulating local electron density, resulting in altered physical or chemical properties.[1−4] Hydrogen bonding in particular has been critical to the development of organocatalysis, where enhanced reactivity or asymmetric transformations may be promoted through hydrogen-bound intermediates.[5] Great advances have been made over several decades, with the design and optimization of new catalysts being guided by experimental and theoretical evaluation of hydrogen bonding networks.[6] Although a hydrogen bond acceptor may be any Lewis basic atom, the very nature of hydrogen bonding limits the hydrogen bond donor to the hydrogen atom. In contrast, electrostatic interactions between a Lewis basic atom and a halogen may provide intermediates of varying physical and chemical properties depending on the size and electronegativity of the halogen in question.[7] Halogen bonding has gained attention as a potential surrogate for hydrogen bonding, and several recent reports demonstrate its utility in promoting organic transformations.[8] Recently, halogen bonding between the fluorine of Selectfluor and electron-rich pyridines has been implicated in generating complexes that participate in single-electron transfer for heterobenzylic radical fluorinations (Scheme 1A).[9] Our concurrent work in this area has suggested that a variety of electronically diverse pyridines interact with Selectfluor to affect Ag(I)-mediated single-electron reduction. We have found that the electronic characteristics of pyridine additives affect the efficiency of benzylic radical fluorination, and counterintuitive trends in product distribution are observed (Scheme 1B).

Scheme 1. Radical Fluorination via Halogen Bonding

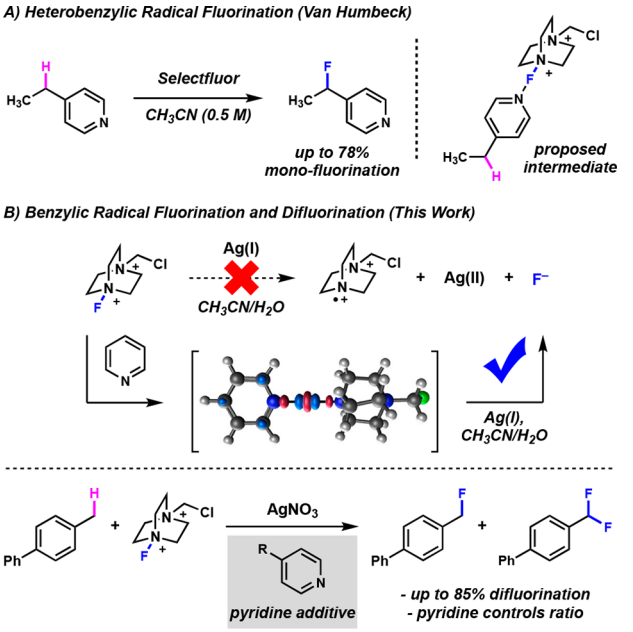

Received: February 11, 2019
Revised: March 8, 2019
Published: March 12, 2019

DOI: 10.1021/acscatal.9b00623
ACS Catal. XXXX, XXX, XXX−XXX

From our previous report on radical fluorination, we concluded that amino acids acted as ligands to lower the oxidation potential of Ag(I) to produce Ag(II) under mild conditions.[10] Binding Ag(I) through an electron-rich nitrogen atom was critical to promote oxidation, with *N*-protected amino acids failing to produce any observed reactivity. We subsequently established that pyridine was a suitable ligand for Ag(I), enabling C−H fluorination from previously ineffective *N*-protected amino acids. Because a wide variety of pyridines are readily available, we became interested in exploring them as additives for our fluorination protocol. Control reactions with 4-methylbiphenyl (**1**) showed that Ag(I), Selectfluor, and pyridine were required for fluorination, but amino acid additives were not (Table 1, entry 4). Reaction in the presence of (2,2,6,6-tetramethylpiperidin-1-yl)oxyl (TEMPO) produced radical-trapped adducts and inhibited fluorination (entry 5).[11] No fluorinated products were observed using *N*-fluoropyridinium tetrafluoroborate as a fluorine source (entry 6), suggesting that fluorine transfer from Selectfluor to pyridine is not the source of reactivity. On the basis of the mechanistic studies of Lectka, we believed pyridine-mediated fluorination occurs via C−H abstraction from the diazabicyclo radical cation **2** formed via single-electron reduction of Selectfluor.[12] This mechanism relies on Ag(I) only as an initiator and does not require a carboxylate to reform Ag(I) via oxidative decarboxylation. In this mechanism, **2** is presumably regenerated via radical fluorination with Selectfluor to continue the radical chain process.

On the basis of these results, we explored a series of 4-substituted pyridines as additives for radical fluorination. Our original hypothesis was that pyridines served to lower the oxidation potential of Ag(I), facilitating electron transfer. Cyclic voltammetry showed that electron-rich pyridines produced Ag(I) species with the lowest oxidation potentials, suggesting facile single-electron transfer to Selectfluor from the electron-rich metal. From these results, we expected a catalyst derived from Ag(I) and 4-methyoxypyridine to be optimum for fluorination. However, we were surprised to find that electron-rich pyridines were the *least* effective at promoting radical fluorination of 4-methylbiphenyl (Scheme 2). Using two equivalents of Selectfluor, a clear trend was observed whereby electron-poor pyridines were the most efficient additives, favoring difluorination as the major product. Experiments using a 5-fold excess of Selectfluor show that difluorination is possible from all pyridines examined. In situ ReactIR suggested that pyridines interact directly with the $[N-F]^+$ bond of Selectfluor, leading us to consider the possibility of halogen bonding as the source of our unexpected reactivity.[11]

Spectroscopic and theoretical work by Erdélyi established pyridines as halogen bond acceptors, and his studies showed that the extent of halogen bonding is affected by pyridine electronics.[13] In that work, diagnostic chemical shifts of pyridine ^{15}N NMR signals were used to infer halogen bonding with *N*-fluoropyridinium, but only minor changes in $[N-^{19}F]^+$ chemical shift were observed under various conditions.[14] Our own in situ NMR studies under synthetic conditions yielded similar results, with negligible shifts observed for the Selectfluor $[N-^{19}F]^+$ signal in the presence of pyridine additives (Table 2). However, we did observe significant changes in pyridine ^{15}N chemical shifts, as measured by $^1H/^{15}N$ HMBC. In all cases examined, pyridine ^{15}N signals shifted to more negative values in the presence of Selectfluor, consistent with the generation of a

Table 1. Discovery of Pyridine-Mediated Fluorination[a]

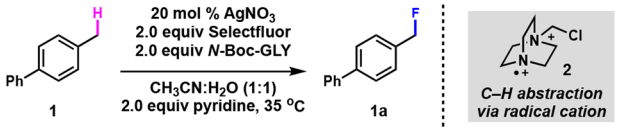

entry	deviation from standard conditions	Yield(%)
1	none	88
2	no $AgNO_3$	00
3	no pyridine	00
4	no *N*-Boc-GLY	51
5	no *N*-Boc-GLY, TEMPO added	*trace*
6	*N*-fluoropyridinium instead of Selectfluor	00

[a]NMR conversion versus 1,3,5-trimethoxybenzene. Standard conditions: 4-methylbiphenyl (**1**) (0.2 mmol), *N*-(*tert*-butoxycarbonyl)-glycine (*N*-Boc-GLY) (0.4 mmol), Selectfluor (0.4 mmol), $AgNO_3$ (0.04 mmol), pyridine (0.2 mmol), 2 mL $CH_3CN:H_2O$ (1:1), 35 °C for 24 h.

Scheme 2. Pyridine-Dependent Product Distribution[a]

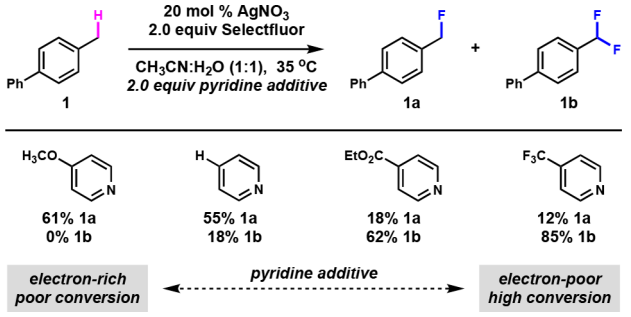

[a]NMR conversion versus 1,3,5-trimethoxybenzene. Conditions: 4-methylbiphenyl (**1**) (0.2 mmol), Selectfluor (0.4 mmol), $AgNO_3$ (0.04 mmol), pyridine (0.2 mmol), 2 mL $CH_3CN:H_2O$ (1:1), 35 °C for 24 h.

Table 2. Chemical Shifts of Pyridines with Selectfluor[‡]

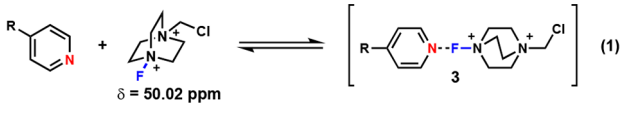

R	^{15}N	^1H (C–2)	^{15}N	^1H (C–2)	^{19}F
CF_3	-67.31	7.95	-68.21	7.93	50.01
CO_2Et	-66.76	7.86	-70.54	7.86	50.03
H	-80.79	7.69	-92.64	7.66	50.01
OCH_3	-102.59	7.51	-153.76[a]	7.49	50.00
	-122.39	7.46	–	–	49.34

[‡]^1H and ^{15}N chemical shifts referenced to nitromethane in a sealed capillary tube. ^{19}F chemical shifts referenced to hexafluorobenzene in a sealed capillary tube. Conditions: pyridine (0.1 mmol,) Selectfluor (0.1 mmol), in 700 uL of $CD_3CN:H_2O$ (1:1) at 25 °C. [a]Averaged value of overlapping signals. Commercial *N*-fluoropyridinium tetrafluoroborate (0.1 mmol), in 700 uL of $CD_3CN:H_2O$ (1:1) at 25 °C is provided as a reference.

DOI: 10.1021/acscatal.9b00623
ACS Catal. XXXX, XXX, XXX−XXX

"pyridinium-like" intermediate. Data for commercial *N*-fluoropyridinium is shown in Table 2 for comparison.

In the case of 4-methoxypridine, a shift of greater than 50 ppm is observed along the ^{15}N axis in the presence of Selectfluor, yielding a broad series of signals that coincides with line broadening of the C−2 ^{1}H NMR signal (Figure 1). In situ

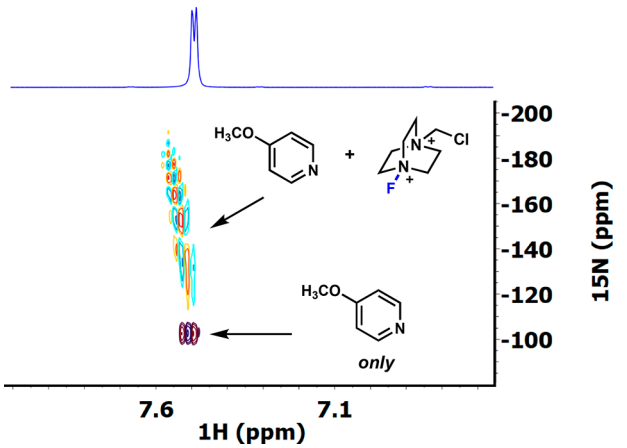

Figure 1. $^{1}H/^{15}N$ coupled HMBC of 4-methoxypyridine alone (maroon, blue) and with Selectfluor (yellow, teal, orange). Conditions: 4-methoxypyridine (0.1 mmol,) Selectfluor (0.1 mmol), in 700 uL CD_3CN/D_2O (1:1) at 25 °C.

ReactIR shows that 4-methoxypyridine consumes Selectfluor under synthetic conditions without Ag(I) present, presumably either via nucleophilic displacement of fluorine or single-electron transfer as proposed by Van Humbeck.[9] Similar effects are observed for pyridine, albeit with a smaller ^{15}N chemical shift and reduced rate of Selectfluor consumption. Interestingly, electron-poor pyridines do not consume Selectfluor in the absence of Ag(I), but exhibit clear interactions as evidenced by ^{15}N NMR and IR spectroscopy.[11] To further investigate the effects of halogen bonding on the efficiency of our radical fluorinations, we pursued computational evaluation of $[N{-}F{-}N]^+$ halogen bound intermediates involving pyridines and Selectfluor.

Computational efforts first involved determining the speciation and chemical properties of Ag(I)/pyridine complexes. Calculations using the B3PW91/6-311G(d) model chemistry including implicit solvation by acetonitrile were carried out using a local development version of Gaussian.[15,16] The calculated Ag(I) oxidation potentials showed that bis-pyridine Ag(I) species are the most likely reductants to initiate radical fluorination.[11] Calculated E^0 values for a series of bis-pyridine Ag(I) adducts were consistent with experimental values measured directly via cyclic voltammetry, confirming that electron-rich pyridines lead to easily oxidized Ag(I) initiators.

With experimental and theoretical results in agreement regarding Ag(I) oxidation, we turned to modeling halogen-bound pyridine/Selectfluor complexes. Preliminary results suggested density functional theory (DFT) model chemistries, including those with empirical dispersion corrections are unable to treat the physics of the $[N{-}F{-}N]^+$ halogen bond. Noting two extensive benchmark reports by Martin and by Wong,[17] indicating only a limited set of approximate functionals are capable of predicting halogen bonding strengths, we suspect our observations are due to the exceptionally electron-deficient character of the $[N{-}F{-}N]^+$ motif. Therefore, we turned to correlated wave function methods. Geometries of candidate halogen-bound species were optimized with the MP2/6-311+G(d) level of theory and single-point energies were evaluated with the CCSD(T)/6-311+G(d) model chemistry including implicit solvation. These calculations identified pyridine/Selectfluor complexes featuring the anticipated $[N{-}F{-}N]^+$ bonding motif (Table 3, eq 1). The halogen-bound

Table 3. Trends for Selectfluor-Pyridine Halogen Bond

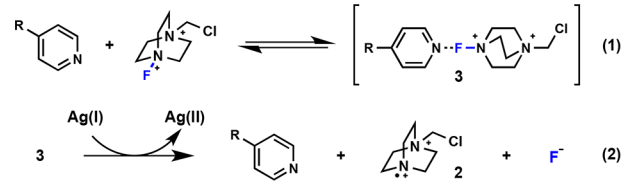

R group	$\Delta H1$ (kcal/mol)	$\Delta H2$ (kcal/mol)
OCH_3	0.34	−31.42
H	0.74	−31.82
CO_2Et	3.63	−33.66
CF_3	2.57	−34.71

species are slightly higher in energy (<1−4 kcal/mol) than the unbound species, though subsequent reduction to form diazabicyclo radical cation **2** is quite favorable (Table 3, eq 2, vide infra).

Computational results suggested that electron-rich pyridines were more effective halogen bond acceptors than electron-deficient pyridines, which agreed with chemical shift data provide in Table 2.[18] As shown in Table 3, the energetics of $[N{-}F{-}N]^+$ bond reduction via single-electron transfer exhibit a clear trend depending on the electronic characteristics of the pyridine. Interestingly, all structures exhibit similar bond lengths for both N−F bonds (~1.84 Å) in the complex and a linear N−F−N bond angle. We were pleased to note that the reduction of the $[N{-}F{-}N]^+$ halogen-bound complex is most energetically favorable with an electron-poor pyridine. These data correlate directly to the experimental reactivity trends observed in Scheme 2, whereby electron-poor pyridines are the most efficient at promoting radical fluorination. Studies exploring alternative bonding interactions, including halogen bonding to the chlorine of Selectfluor, showed the only suitable geometry is as shown in structure **3**. In addition, because synthetic experimental conditions include water as a cosolvent, the possibility of a mixed hydrogen/halogen bonding network was also explored computationally.[11] The inclusion of discrete water molecules into complex **3** did not converge into meaningful structures, suggesting the effects reported in Table 2 are the result of direct interaction between the pyridine nitrogen and Selectfluor $[N{-}F]^+$.

Exploring the extent to which post-SCF correlation affects the electron density to give rise to the $[N{-}F{-}N]^+$ weak interaction, we evaluated the difference between MP2 and reference Hartree−Fock electron densities. Scheme 1B shows such a depiction for **3**. Electron correlation yields symmetric redistribution of electron density in the two N−F bonding regions, which is consistent with our analysis that post-SCF treatment is required to properly account for the $[N{-}F{-}N]^+$ weak interactions.

To further explore the effects of pyridine/Selectfluor interactions in the context of radical initiation, we examined the electrochemical reduction of Selectfluor under synthetic

DOI: 10.1021/acscatal.9b00623
ACS Catal. XXXX, XXX, XXX−XXX

conditions. As shown in Scheme 3, Selectfluor produces an irreversible single-electron reduction at approximately −1.18 V.

Scheme 3. Electrochemical Reduction of Selectfluor[a]

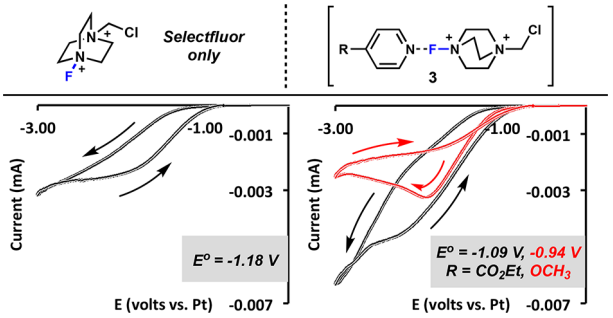

[a]Conditions: Selectfluor (0.5 mmol) in 5 mL of CH_3CN:H_2O (1:1), tetrabutylammonium tetrafluoroborate supporting electrolyte (0.1 M), pyridine (where applicable) (0.5 mmol). Left: Selectfluor alone (black curve). Right: Selectfluor with ethyl isonicotinate (black curve), and 4-methoxypyridine (red curve). Arrows indicate the direction of applied potential. E^0 values are determined as the minimum voltage producing −100 μA of current in the reducing direction.

This value was clearly perturbed by the presence of pyridine additives to yield species that reduce at lower potentials than Selectfluor alone, consistent with the energies calculated for $\Delta H2$ in Table 3 above.

On the basis of our combined experimental and computational results, we propose the following mechanism for radical C−H fluorination with Selectfluor via Ag(I)/pyridine initiators (Scheme 4). Analytical electrochemistry and computations

Scheme 4. Proposed Mechanism

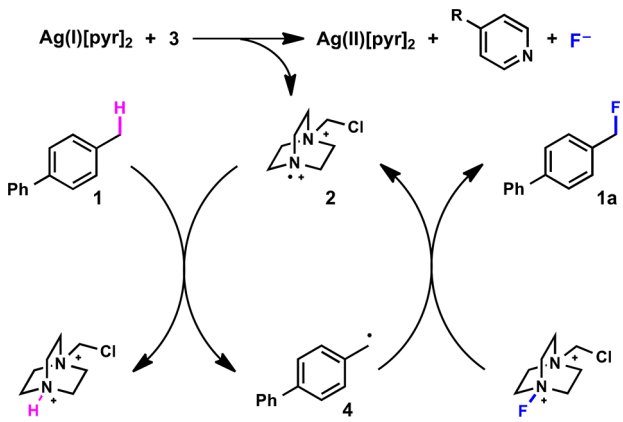

demonstrate that Ag(I)/pyridine complexes are better reductants than Ag(I) alone, suggesting a pre-equilibrium to bis-pyridine Ag(I) complexes. Single-electron transfer to a halogen-bound pyridine/Selectfluor complex **3** would produce Ag(II)-$[pyr]_2$, pyridine, fluoride anion, and diazabicyclo radical cation **2**. C−H abstraction of **1** produces nucleophilic radical **4** that quenches with an additional equivalent of Selectfluor to regenerate **2**, propagating the radical reaction. At this stage of investigation, it is unclear whether halogen-bonding is *required* for Selectfluor reduction, or if all Ag(I)$[pyr]_2$ initiators investigated are sufficiently reducing to produce **2**. One contributing factor to the marked difference in efficiency shown in Scheme 2 is unproductive consumption of Selectfluor from electron-rich pyridines. However, it cannot be the only factor affecting reaction efficiency, as the trend correlating pyridine electronics to efficiency holds for pyridines that do not affect the concentration of Selectfluor in an unproductive manner.

In conclusion, we have demonstrated experimental and theoretical evidence supporting the presence of halogen bonding in pyridine-mediated radical fluorinations. Two-dimensional NMR shows clear ^{15}N shifts of pyridine additives when exposed to Selectfluor under synthetic conditions. Counterintuitive trends in reaction efficiency are rationalized via computational modeling of $[N-F-N]^+$ intermediates and in situ reaction monitoring, leading to a clearer picture of electron transfer between Ag(I)$[pyr]_2$ initiators and Selectfluor in the presence of pyridine. Analytical electrochemistry shows that pyridine additives affect the single-electron reduction of Selectfluor, consistently producing species that are more easily reduced. A comprehensive mechanistic picture of radical fluorination likely involves equilibration of pyridine with both Ag(I) and Selectfluor, leading to a complicated kinetic scenario that we are currently studying via in situ reaction monitoring and computational modeling.

■ ASSOCIATED CONTENT

Supporting Information

The Supporting Information is available free of charge on the ACS Publications website at DOI: 10.1021/acscatal.9b00623.

Computational procedures, optimized geometries, and the full Gaussian citation (PDF)

General considerations and reaction procedures and supplemental data (PDF)

■ AUTHOR INFORMATION

Corresponding Authors

*E-mail: hhratchian@ucmerced.edu.

*E-mail: rbaxter@ucmerced.edu.

ORCID

Hrant P. Hratchian: 0000-0003-1436-5257

Ryan D. Baxter: 0000-0002-1341-5315

Author Contributions

†(A.M.H., S.L.B.) These authors contributed equally to this work.

Notes

The authors declare no competing financial interest.

■ ACKNOWLEDGMENTS

S.L.B. acknowledges the faculty mentor fellowship program at UC Merced. H.P.H. acknowledges the ACS-PRF No. 56806-DNI6, computing time on the MERCED cluster supported by the National Science Foundation under Grant No. ACI-1429783, and the Hellman Fellows Fund for a faculty fellowship. R.D.B. acknowledges the ACS-PRF No. 56225-DNI5. This material is based upon work supported by the National Science Foundation under Grant No. 1752821 (R.D.B.). We thank Dave Rice for his help in the acquisition and interpretation of NMR spectra.

■ REFERENCES

(1) Parsegian, V. A. *Van der Waals Forces: A Handbook for Biologists, Chemists, Engineers, and Physicists*; Cambridge University Press: Cambridge and New York, 2006; pp 41−98.

DOI: 10.1021/acscatal.9b00623
ACS Catal. XXXX, XXX, XXX−XXX

(2) (a) Hunter, C. A.; Sanders, J. K. M. The Nature of π-π Interactions. *J. Am. Chem. Soc.* **1990**, *112*, 5525−5534. (b) Neel, A. J.; Hilton, M. J.; Sigman, M. S.; Toste, F. D. Exploiting Non-Covalent π Interactions for Catalyst Design. *Nature* **2017**, *543*, 637−646.

(3) (a) Frontera, A.; Gamez, P.; Mascal, M.; Mooibroek, T. J.; Reedijk, J. Putting Anion-π Interactions into Perspective. *Angew. Chem., Int. Ed.* **2011**, *50*, 9564−9583. (b) Mahadevi, A. S.; Sastry, G. N. Cation-π Interaction: Its Role and Relevance in Chemistry, Biology, and Material Science. *Chem. Rev.* **2013**, *113*, 2100−2138.

(4) (a) Jeffrey, G. A. *An Introduction to Hydrogen Bonding*; Oxford University Press: New York, 1997, Vol. *4*, p 303. (b) Grabowski, S. *Chem. Rev.* **2011**, *111*, 2597−2625.

(5) Doyle, A. G.; Jacobsen, E. N. Small-Molecule H-Bond Donors in Asymmetric Catalysis. *Chem. Rev.* **2007**, *107*, 5713−5743.

(6) (a) Hamza, A.; Schubert, G.; Soos, T.; Papai, I. Theoretical Studies on the Bifunctionality of Chiral Thiourea-Based Organocatalysts: Competing Routes to C−C Bond Formation. *J. Am. Chem. Soc.* **2006**, *128*, 13151−13160. (b) Armstrong, A.; Boto, R. A.; Dingwall, P.; Contreras-Garcia, J.; Harvey, M. J.; Mason, N. J.; Rzepa, H. S. The Houk-List Transition States for Organocatalytic Mechanisms Revisited. *Chem. Sci.* **2014**, *5*, 2057−2071. (c) Zabka, M.; Sebesta, R. Experimental and Theoretical Studies of Hydrogen-Bonding in Organocatalysis. *Molecules* **2015**, *20*, 15500−15524. (d) Grayson, M. N. Mechanism and Origins of Stereoselectivity in the Cinchona Thiourea- and Squaramide-Catalyzed Asymmetric Michael Addition of Nitroalkanes to Enones. *J. Org. Chem.* **2017**, *82*, 4396−4401.

(7) Desiraju, G. R.; Ho, P. S.; Kloo, L.; Legon, A. C.; Marquardt, R.; Metrangolo, P.; Politzer, P.; Resnati, G.; Rissanen, K. Definition of the halogen bond (IUPAC Recommendations 2013). *Pure Appl. Chem.* **2013**, *85*, 1711−1713.

(8) (a) Nagorny, P.; Sun, Z. New approaches to organocatalysis based on C−H and C−X bonding for electrophilic substrate activation. *Beilstein J. Org. Chem.* **2016**, *12*, 2834−2848. (b) Guha, S.; Kazi, I.; Nandy, A.; Sekar, G. Role of Lewis-Base-Coordinated Halogen(I) Intermediates in Organic Synthesis: The Journey from Unstable Intermediates to Versatile Reagents. *Eur. J. Org. Chem.* **2017**, *2017*, 5497−5518. (c) Chen, M.-W.; Ji, Y.; Wang, J.; Chen, Q.-A.; Shi, L.; Zhou, Y.-G. Asymmetric Hydrogenation of Isoquinolines and Pyridines Using Hydrogen Halide Generated in Situ as Activator. *Org. Lett.* **2017**, *19*, 4988−4991. (d) Ma, R.; He, L.-N.; Liu, X.-F.; Liu, X.; Wang, M.-Y. DBU as Activator for the *N*-iodosuccinimide Promoted Chemical Fixation of Carbon Dioxide with Epoxides. *Journal of CO_2 Utilization* **2017**, *19*, 28−32. (e) Kobayashi, Y.; Nakatsuji, Y.; Li, S.; Tsuzuki, S.; Takemoto, Y. Direct *N*-Glycofunctionalization of Amides with Glycosyl Trichloroacetimidate by Thiourea/Halogen Bond Donor Co-Catalysis. *Angew. Chem., Int. Ed.* **2018**, *57*, 3646−3650. (f) Lu, Y.; Nakatsuji, H.; Okumura, Y.; Yao, L.; Ishihara, K. Enantioselective Halo-oxy- and Halo-azacyclizations Induced by Chiral Amidophosphate Catalysts and Halo-Lewis Acids. *J. Am. Chem. Soc.* **2018**, *140*, 6039−6043. (g) Brückner, R.; Haller, H.; Steinhauer, S.; Müller, C.; Riedel, S. A 2D Polychloride Network Held Together by Halogen-Halogen Interactions. *Angew. Chem., Int. Ed.* **2015**, *54*, 15579−15583. (h) Riedel, S.; Köchner, T.; Wang, X.; Andrews, L. Polyfluoride Anions, a Matrix-Isolation and Quantum-Chemical Investigation. *Inorg. Chem.* **2010**, *49*, 7156−7164. (i) Gliese, J.; Jungbauer, S. H.; Huber, S. M. A Halogen-Bonding-Catalyzed Michael Addition Reaction. *Chem. Commun.* **2017**, *53*, 12052−12055. (j) Heinen, F.; Engelage, E.; Dreger, A.; Weiss, R.; Huber, S. M. Iodine(III) Derivatives as Halogen Bonding Organocatalysts. *Angew. Chem., Int. Ed.* **2018**, *57*, 3830−3833. (k) Schindler, S.; Huber, S. M. Halogen Bonds in Organic Synthesis and Organocatalysis. In *Halogen Bonding II: Impact on Materials Chemistry and Life Sciences*; Metrangolo, P., Resnati, G., Eds.; Springer International Publishing: Cham, 2015; Vol. *359*, pp 167−204. (l) Breugst, M.; von der Heiden, D. Mechanisms in Iodine Catalysis. *Chem. - Eur. J.* **2018**, *24*, 9187. (m) von der Heiden, D.; Detmar, E.; Kuchta, R.; Breugst, M. Activation of Michael Acceptors by Halogen-Bond Donors. *Synlett* **2018**, *29*, 1307−1313. (n) Breugst, M.; von der Heiden, D.; Schmauck, J. Novel Noncovalent Interactions in Catalysis: A Focus on Halogen, Chalcogen, and Anion-n Bonding. *Synthesis* **2017**, *49*, 3224−3236.

(9) Danahy, K. E.; Cooper, J. C.; Van Humbeck, J. F. Benzylic Fluorination of Aza-Heterocycles Induced by Single-Electron Transfer to Selectfluor. *Angew. Chem., Int. Ed.* **2018**, *57*, 5134−5138.

(10) Hua, A. M.; Mai, D. N.; Martinez, R.; Baxter, R. D. Radical C−H Fluorination Using Unprotected Amino Acids as Radical Precursors. *Org. Lett.* **2017**, *19*, 2949−2952.

(11) See Supporting Information for further details.

(12) (a) Pitts, C. R.; Bloom, S.; Woltornist, R.; Auvenshine, D. J.; Ryzhkov, L. R.; Siegler, M. A.; Lectka, T. Direct, Catalytic Monofluorination of sp^3 C−H Bonds: A Radical-Based Mechanism with Ionic Selectivity. *J. Am. Chem. Soc.* **2014**, *136*, 9780−9791. (b) Pitts, C. R.; Ling, B.; Woltornist, R.; Liu, R.; Lectka, T. Triethylborane-Initiated Radical Chain Fluorination: A Synthetic Method Derived from Mechanistic Insight. *J. Org. Chem.* **2014**, *79*, 8895−8899.

(13) (a) Carlsson, A.-C. C.; Veiga, A. X.; Erdélyi, M. Halogen Bonding in Solution. In *Halogen Bonding II: Impact on Materials Chemistry and Life Sciences*; Metrangolo, P., Resnati, G., Eds.; Springer International Publishing: Cham, 2015; Vol. *359*, pp 49−76. (b) Bedin, M.; Karim, A.; Reitti, M.; Carlsson, A.-C. C.; Topic, F.; Cetina, M.; Pan, F.; Havel, V.; Al-Ameri, F.; Sindelar, V.; Rissanen, K.; Grafenstein, J.; Erdelyi, M. Counterion Influence on the N−I−N Halogen Bond. *Chem. Sci.* **2015**, *6*, 3746−3756. (c) Carlsson, A.-C. C.; Mehmeti, K.; Uhrbom, M.; Karim, A.; Bedin, M.; Puttreddy, R.; Kleinmaier, R.; Neverov, A. A.; Nekoueishahraki, B.; Gräfenstein, J.; Rissanen, K.; Erdélyi, M. Substituent Effects on the $[N{-}I{-}N]^+$ Halogen Bond. *J. Am. Chem. Soc.* **2016**, *138*, 9853−9863.

(14) Karim, A.; Reitti, M.; Carlsson, A.-C. C.; Grafenstein, J.; Erdelyi, M. The Nature of $[N{-}Cl{-}N]^+$ and $[N{-}F{-}N]^+$ Halogen Bonds in Solution. *Chem. Sci.* **2014**, *5*, 3226−3233.

(15) Frisch, M. J.; Trucks, G. W.; Schlegel, H. B.; Scuseria, G. E.; Robb, M. A.; Cheeseman, J. R.; Scalmani, G.; Barone, V.; Petersson, G. A.; Nakatsuji, H.; Li, X.; Caricato, M.; Marenich, A. V.; Bloino, J.; Janesko, B. G.; Gomperts, R.; Mennucci, B.; Hratchian, H. P.; Ortiz, J. V.; Izmaylov, A. F.; Sonnenberg, J. L.; Williams-Young, D.; Ding, F.; Lipparini, F.; Egidi, F.; Goings, J.; Peng, B.; Petrone, A.; Henderson, T.; Ranasinghe, D.; Zakrzewski, V. G.; Gao, J.; Rega, N.; Zheng, G.; Liang, W.; Hada, M.; Ehara, M.; Toyota, K.; Fukuda, R.; Hasegawa, J.; Ishida, M.; Nakajima, T.; Honda, Y.; Kitao, O.; Nakai, H.; Vreven, T.; Throssell, K.; Montgomery, J. A., Jr.; Peralta, J. E.; Ogliaro, F.; Bearpark, M. J.; Heyd, J. J.; Brothers, E. N.; Kudin, K. N.; Staroverov, V. N.; Keith, R.; Kobayashi, J.; Normand, K.; Raghavachari, A. P.; Rendell, J. C.; Burant, S. S.; Iyengar, J.; Tomasi, M.; Cossi, J. M.; Millam, T. A.; Klene, M.; Adamo, C.; Cammi, R.; Ochterski, J. W.; Martin, R. L.; Morokuma, K.; Farkas, O.; Foresman, J. B.; Fox, D. J.; *Gaussian*, Development Version, Revision I.10+; Gaussian, Inc.: Wallingford, CT, 2016.

(16) (a) Becke, A. D. Density-functional thermochemistry. III. The role of exact exchange. *J. Chem. Phys.* **1993**, *98*, 5648. (b) Wang, Y.; Perdew, J. P. Spin scaling of the electron-gas correlation energy in the high-density limit. *Phys. Rev. B: Condens. Matter Mater. Phys.* **1991**, *43*, 8911.

(17) (a) Kozuch, S.; Martin, J. M. L. Halogen Bonds: Benchmarks and Theoretical Analysis. *J. Chem. Theory Comput.* **2013**, *9*, 1918−1931. (b) Anderson, L. N.; Aquino, F. W.; Raeber, A. E.; Chen, X.; Wong, B. M. Halogen Bonding Interactions: Revised Benchmarks and a New Assessment of Exchange vs Dispersion. *J. Chem. Theory Comput.* **2018**, *14*, 180−190.

(18) Correlation of computed binding constants to ^{1}H-NMR chemical shifts was attempted using the web-based software at www.app.supramolecular.org/bindfit/. These results are provided in the Supporting Information.

DOI: 10.1021/acscatal.9b00623
ACS Catal. XXXX, XXX, XXX−XXX